Dissipated Energy-Based Analysis of Fatigue Behavior of Hot-Mix Asphalt

Pyeong-Jun Yoo, Byung-Sik Um, Ji-Young Choi, Yeon-Bok Kim
Highway Research Division
Korea Institute of Construction Technology
2311 Simin-Daero, Ilsan, Goyang, Korea
pjyoo@kict.re.kr, bseom@kict.re.kr,legion@kict.re.kr, ybkim@kict.re.kr

ABSTRACT

The allowable number of loading cycle up to the 50 % loss of the initial flexural stiffness (N_f-50%) of Hot-Mix Asphalt (HMA) is widely accepted as a fatigue failure criterion. However, the cyclic load-induced fatigue damage may not be explained by the N_f-50% criterion because it is difficult to recognize the phenomenological threshold between the elastic range without any noticeable crack or macro damage and the plastic range where macro cracks initiates during loading cycles. The cyclic load-induced fatigue crack of HMA is the process by which the pavement deteriorates through cracking or irrecoverable plastic strains are accumulated by repetitive loading. Along this process, phenomenological fatigue behaviors under a cyclic loading amplitude are classified into three stages during a period of loading, the primary stage (high dissipated strain energy-change without any crack or macro damage), the secondary stage (constant dissipated strain energy-change between two consecutive hysteresis loading loop), and the tertiary stage (rapid-change of the dissipated strain energy). The threshold between the secondary stage and the tertiary stage is proposed as a fatigue failure criterion not by the N_f-50% criterion in this study. The fatigue behavior of HMA under various cyclic loading amplitudes is characterized by the dissipated energy change. This study clarifies the dissipated energy-changes during the whole loading cycles for the 13mm dense-graded HMA using four-point bending tests at various strain amplitudes (200$\mu\varepsilon$-800$\mu\varepsilon$) under strain-controlled modes at 20°C in this study.

1. INTRODUCTION

Hot-Mix Asphalt (HMA) is a composite mixture, composed of aggregate, asphalt binder, and filler. Although each component of HMA exhibits different mechanistic behavior under a specific loading condition, a mechanistic behavior of HMA is usually characterized on assumptions of a continuum media like homogeneous and isotropic one regardless of mechanistic models or fatigue damage models. With these assumptions, one of mechanistic analogues amongst elastic, visco-elastic, or visco-elasto-plastic is usually utilized to derive a constitutive model of HMA. This means that the mechanistic behavior of HMA may not be modeled with a single term of mechanistic analog like an elastic spring, a viscous dashpot, or a plastic slider.[1]

Regardless of these concerns, most methods for determination of material properties continue to use linear elastic assumptions for thickness design of HMA due to complications of introducing visco-elastic, visco-plastic, or nonlinearity. Similarly, in the process of fatigue damage model of HMA, it is usually utilizes phenomenological results like loading and displacement to construct a fatigue damage model which is different with the mechanistic model defining a relationship between stress and strain.[1][2]

Although a constitutive model of HMA is an essential component in a mechanistic pavement design procedure, a fatigue failure criterion should also be introduced for the performance life prediction of HMA. An allowable load repetition with fatigue damage is usually defined by using a fatigue failure criterion of the 50 % loss of initial flexural stiffness of HMA(N_f-50%) under a cyclic loading condition.[3]

However, noticeable macro damage or crack during whole loading cycles may not be clearly explained with the 50% of initial stiffness-loss criterion because there is only a conceptual limit

not a physical parameter to explain the threshold between the elastic range without any crack and the plastic behavior where irreversible crack initiated during loading cycles.

The fatigue failure of HMA may be the threshold where the pavement deteriorates through macro cracking because irrecoverable strains are accumulated by repeated loadings over time. The phenomenological fatigue behavior, which is the dissipated strain energy changes versus loading cycles, was classified into the three stages during a period of cyclic loading, the primary stage (high strain energy-change without any noticeable crack), the secondary stage (constant strain energy-change between two consecutive hysteresis loop), and the tertiary stage (rapid change of strain energy) for the HMA mixture under various strain amplitudes.[4][5]

Various arbitrary numbers of loading cycles nearby the onset of the tertiary stage of each test are utilized to make a plot of strain amplitudes versus the number of loading cycles at failure, ε_a-N_f curve in this study.

This study addresses that conventional fatigue analysis approaches using N_f-50% rule may be lacking in providing a physical picture of asphalt mixture's phenomenological damage mechanism (crack initiation and propagation).

In addition, the loading condition in this study still causes the fatigue life of laboratory specimens to be shorter than the life expected in the field. In the future, as a consecutive research on this issue, the effects of temperature, loading frequency, mixture types, and rest periods will be addressed in fatigue evaluation by incorporating a new fundamental measure into the fatigue damage prediction model which is developed in this study.

2. PHEONOMENOLOGICAL FATIGUE DAMAGE OF HMA

Fatigue damage to the HMA caused by cyclic stresses and strains due to load-induced (traffic loading) or non-load induced (temperature changes) factors is one of the primary distress mode in asphalt pavements.

The main goal of this study is to evaluate the effect of cyclic loading on HMA's fatigue damages. According to the specific loading condition either a displacement-controlled or a force-controlled, it is possible to evaluate the aggressiveness of the loading as it applies over the HMA specimen.

Following sections describe a laboratory test, fatigue damage mechanism associated with pavement distresses like cracks and current adoptive transfer functions to calculate the allowable number of loading repetitions to fatigue failure.

In a widely accepted fatigue damage mechanism, maximum tensile strains at the bottom of HMA are usually used to determine fatigue damage, which is generally caused by repeated heavy axle loads. It is cumulative localized damages due to a build-up of irrecoverable strains. The location where fatigue cracking potential is the highest has generally been thought at the bottom of HMA, where critical tensile strain may exist.[2][3][4]

Several models are available to predict fatigue life of HMA from the tensile strain at the bottom of HMA. However, it is hard to measure the tensile strains at the bottom of HMA specimen in the laboratory directly so that the four-point bending beam fixture is usually utilized for characterizing the fatigue behavior of HMA under the displacement-controlled mode in the mid-point of a specimen.[3][4]

Four-Point Bending Beam Fatigue Test

The four-point bending beam test (4PB) is a global method for the characterization of fatigue behavior of HMA rather than analyzing the constituent modeling of HMA. The 4PB has the advantage of providing a constant bending moment and zero-shear over the length of the specimen. This assumed that the deflection due to the shear is neglected; then, this produces uniform bending in the central third of the specimen and simplifies analysis.[6]

The 4PB applies loading at inner clamps located at one-third distances from the beam ends, at which X=A and X=B shown in Figure 1. The specimen is repeatedly loaded, either in displacement- or force-controlled mode until a predefined failure occurs like the N_f-50% rule or until meets the tertiary stage in this study.

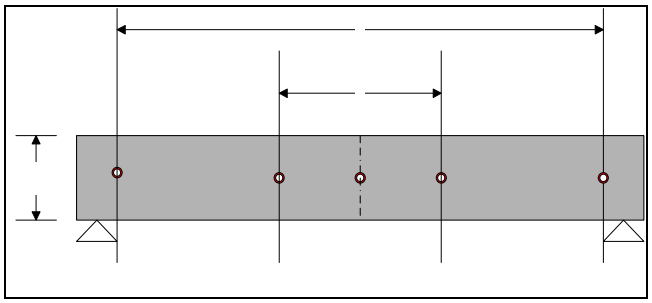

Figure 1. Four-point bending beam test specimen [6]

The common calculation procedure in the measurements through the specimen as Figure1 is following:[6]

$$\varepsilon_{\max} = \frac{12h}{3L^2 - 4a^2} V_{\max} \tag{1}$$

where

ε_{max} = maximum tensile strain, mm/mm,

V_{max} = maximum deflection in the center of the beam, mm, and

h, L, and a = beam dimension, see Figure 1

The maximum bending stress is given by:

$$\sigma_{\max} = \frac{3a}{bh^2} F_0 \tag{2}$$

where

σ_{max} = maximum bending stress, MPa

F_0 = Load, N, and

b = beam width, mm

Stiffness modulus is calculated as follows:

$$K = \frac{\sigma_{max}}{\varepsilon_{max}} \tag{3}$$

where

K is the beam stiffness in MPa, and

ε_{max} = maximum tensile strain

The phase angle is expressed as:

$$\phi = 360 \cdot f \cdot s \tag{4}$$

where

ϕ = phase angle, degree,

f = load frequency, Hz, and

s = time lag between displacement and load, sec.

SHRP(Strategic Highway Research Program in USA) also adopts same calculation procedures above to characterize the fatigue behavior of a HMA mixture within a time period using the 4PB test. This procedure recommends four specimens with three replicates tested at least four strain levels to determine the fatigue characteristics of the mixture. The strain levels are arbitrarily chosen such that the fatigue life ranges from approximately 5,000 to 500,000 cycles. All tests are performed in the vertical displacement-controlled mode of loading at a loading frequency of 10Hz. Results from the tests are utilized to derive a plot of strain amplitudes versus loading cycles to the failure, ε_a versus N_f, and fatigue damage characterization by calculating resulting stresses, strains, stiffness, and dissipated energy at the predefined loading cycle interval which is usually 10 cycles.[7][8]

Y=h

The 4PB test runs until the physical failure via crack occurs. However, it usually takes a very long time of loading cycles to reach a physical failure via fracture in relatively low strain amplitudes such as 100-200με. Therefore, to finish a set of 4PB test within a working-day (4 specimens with 4 different strain levels respectively), the specifications (AASHTO TP8-94 and SHRP M-009) set the criteria for the fatigue failure when there is a 50% reduction in the initial stiffness measured after 50 applied load cycles, although there is dispute concerning the definition of failure for the controlled strain test.[7][8]

This study introduces an alternative methods to this issue, each of the tests runs until showing all three fatigue stages, i.e., the primary, the secondary, and the tertiary stages aforementioned in a period of loading time within a day with the range of strain amplitudes about 200με~800με. The fatigue failure was then defined at the threshold between the secondary and the tertiary stage, which has been defined by the ratio of dissipated energy change, although this method has not been fully validated for various mixtures except the 13mm dense-graded HMA in this study.

To investigate the fatigue behavior of HMA, the beam fatigue test set-up in this paper summarized as Table 1.

Table 1. 4PB Beam fatigue test factorial for the 13mm dense-graded HMA

Asphalt Binder	1	PG64-22
Aggregate	1	Nominal maximum aggregate size 13mm
Asphalt content	1	5%
Target Air-Void	1	4%
Maximum Strain levels(με)	4	200, 400, 600, 800
Replicates	4	A1, A2, A3, A4
Loading Frequency	1	10 Hz no rest period-Sinusoidal
Specimen size	1	51cm height × 63.5cm width × 381cm Length
Total Specimens Tested	20	Including 4 dummies

Conventional Fatigue Damage Criteria

If the tensile strain at the bottom of HMA is utilized, the fatigue damage function is generally described as follows:

$$N_f = f_1(\varepsilon_t)^{-f_2}(E_1)^{-f_3} \quad (5)$$

Where

N_f = Allowable Load repetitions,

ε_t = Horizontal tensile strain at the bottom of HMA,

E_1 = Elastic modulus of HMA (psi), and

f_1, f_2, f_3 : Constants determined from laboratory fatigue test.

Since pavement fatigue damage is usually treated as a bottom-up failure mechanism, the crack propagates through the entire HMA layers before appearing at the surface. Therefore, the criticality of this distress is more pronounced in flexible pavements surfaced with a thin to medium-thickness of the HMA layer (less than 100 mm). In the Asphalt Institute (AI) pavement design method, the allowable number of load repetitions to cause fatigue cracking is associated with the critical horizontal tensile strain at the bottom of HMA. The AI (1982) developed fatigue damage model for the 20% of cracked-area is as following transfer function:[10][11]

$$N_f = 0.0796(\varepsilon_t)^{-3.291}(E_t)^{-0.854} \quad (6)$$

where

N_f = allowable number of 18-kip equivalent single axle loads (ESAL),

ε_t = horizontal tensile strain at the bottom of HMA, and

E_t = resilient modulus of HMA (psi).

It is worth noting that all the conventional fatigue damage criteria are usually developed on the basis of the failure criterion of the reduction of 50% of initial stiffness of HMA, i.e., N_f-50% criterion.

In addition, the only target of the conventional approach is to make a fatigue life transfer function through the multi-variable regression technique. No approaches consider a process to classify the HMA as either the brittle or the ductile behavior by arbitrarily defined fatigue parameters relatively.

On the other hand, this study presents that the conventional N_f-50% failure criterion is not valid for all the phenomenological fatigue behavior of HMA specimens, and proposes an alternative method to verify the fatigue failure of HMA specimens.

Conventional Data Analysis

A conventional fatigue analysis was performed using analysis the regression technique. Although the conventional fatigue analysis generally assumes the normally distributed variables; however, it is reported in the literatures that log-normally distributed fatigue data are utilized to make a fatigue life transfer function, and thus the log-transformed data of the 13mm dense-graded HMA was used for analysis in this study. [9][11][12]
The summary of fatigue testing results is as Table 2.

Table 2. Summary of the Test Results

Specimens	Cycles to the Failure	Stress(N/mm^2)	Strain (microStrain)	Initial Flexural Stiffness (N/mm^2)	CDE (N-mm/mm^3)
I4B1S1R1	1,500	1.33	751.2	3171.5	3.15
I4B1S2R2	2,200	1.24	749.9	3263.8	4.50
I4B1S4R4	1,500	1.36	747.2	3372.2	3.15
I3B3S1R1	1,900	1.45	587.3	3201.1	2.33
I3B3S2R2	2,300	1.44	585.4	3334.1	2.92
I3B3S3R3	10,000	1.12	495.7	3493.6	8.82
I3B3S4R4	8,500	1.00	500.2	3438.1	7.49
I2B4S2R2	48,900	0.64	329.9	3602.5	17.63
I2B4S3R3	37,400	0.79	330.3	3473.8	13.51
I2B4S4R4	46,000	0.71	328.2	3369.2	16.60
I1B2S1R1	315,800	0.59	246.1	3627.6	57.75
I1B2S3R3	373,100	0.55	248.9	3408.9	67.52
I1B2S4R4	361,500	0.55	243.4	3734.1	65.62
I15B4S3R3	366,800	0.53	236.1	4094.6	65.75
I15B1S2R2	169,200	0.56	237.7	4047.1	30.60
I20B2S3R1	52,600	0.63	319.3	3669.0	19.23
I30B1S3R1	7,900	1.01	496.9	3545.7	6.77
I30B3S3R2	8,200	1.19	488.2	3810.4	7.17
I35B2S1R2	4,600	1.25	575.5	3410.2	5.63
I35B2S2R3	3,100	1.43	574.9	3466.1	4.49
I45B3S1R1	1,200	1.53	741.8	3397.7	2.47
I45B3S2R2	1,100	1.87	742.2	3503.6	2.35

*CDE: Cumulative Dissipated Energy

Regressions were conducted in the following forms and result in Table 3;

$$ln(N_f) = a + b \cdot ln(\varepsilon_a) \quad (7)$$

$$ln(N_f) = a + b \cdot ln(\varepsilon) + c \cdot ln(S_0) \quad (8)$$

where

N_f = Number of loading repetitions to fatigue failure,

ε_a = applied strain,

S_0 = initial mixture stiffness, and

a, b, and c = regression coefficients.

Table 3. Summary of the Regression Analysis

Model	$ln(N_f) = a+b*ln(\varepsilon)$				
Frequency	a	b	c	RMSE	adjusted R^2
10 Hz	38.632	-4.773	-	0.35	0.972
Model	$ln(N_f) = a+b*ln(\varepsilon)+c*ln(S_0)$				
Frequency	a	b	c	RMSE	adjusted R^2
10 Hz	42.538	-4.819	-0.443	0.36	0.972

Equation 7 and Equation 8 were introduced by Wöhler(1860) and Monismith et al. (1985), those are commonly accepted as a suitable relationship for fatigue, including the strain amplitude and stiffness in a fixed loading frequency (10 Hz) in this study.

The RMSE and adjusted R^2 values for the models are, respectively, 0.35 and 97.2%; 0.36 and 97.2%. The Equation 7 and 8 may be utilized for the prediction of fatigue life from the applied strain for the HMA in this study. However, first, it may be seen that the inclusion of additional variable like the stiffness-term(S_0) is not improving the model significantly in this study (Figure 2), although it needs further tests on additional HMA mixtures to support this more clearly. And secondly, the predictions from the Equation 7 and 8 are not fully covered the whole range of the number of loading cycles to the failure as shown in Figure 2 causing the limiting number of observations, 22 tests in this study.

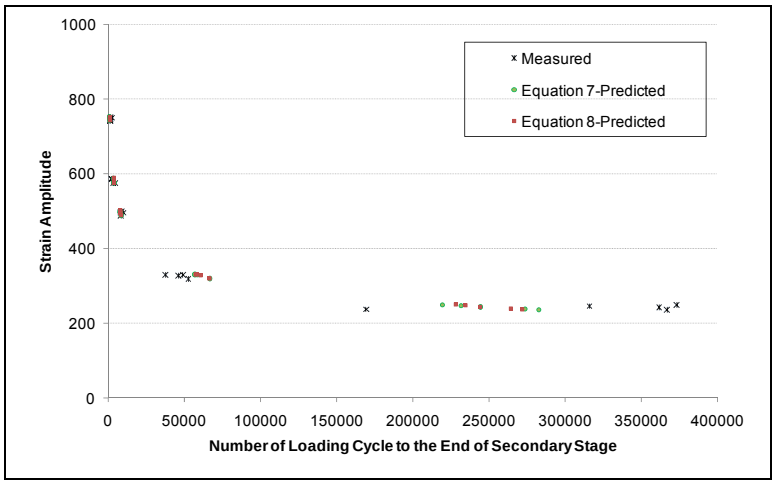

Figure 2. Conventional Fatigue life Prediction: 13mm-dense Grade HMA in this study

The background of the conventional fatigue life prediction models aforementioned may need to have the constitutive assumption that the relationship between stresses and strains of the 4PB test is linearly proportional to each other. Thus, those phenomenological models take either stress-term or strain-term as an independent variable with the N_f-50% as the dependent variable in each transfer functions. However, although the linear relationship of stress and strain may only valid at the relatively low temperature of the HMA specimen such as less than 5°C, it is worth noting that the temperature-dependency of the HMA specimen at the relatively high temperature like above 20°C may not linearly proportional each other between stresses and strains.

To propose a more explainable phenomenological fatigue behavior of the HMA to the whole range of the number of loading cycles to the fatigue failure considering the temperature dependency separately, an alternative method is to be considered in the following section.

3. LOW AND HIGH CYCLE FATIGUE APPROACH

Current flexible pavement design is usually considering the fatigue damage as a main failure mode. In most of fatigue damage analyses for the HMA, many engineers were mainly interested in the S-N (stress versus number of loading cycles) or ε-N (strain versus number of loading cycles) curves depending on the modes of controlled-loading in determining the fatigue endurance limit for the HMA under the regime of high-cycle fatigue (HCF), e.g., greater than 5,000 loading cycles which is based on the SHRP specification.[13]

A special interest occurred in studying low-cycle fatigue (LCF) behavior in the late of 1970s. In the sense of that the materials may fail in both domains in similar manners (LCF tests with relatively high strain amplitudes and HCF tests in relatively low strain amplitudes).

The fatigue damages occur when the HMA is subject to alternating stress due to vehicular loadings over a long period of time. Either the low or the high repeated cyclic loading over the pavements that causes significant plastic damages in the HMA may cause fatigue cracking.

To estimate the fatigue life of the HMA in both regimes, the 4PB fatigue test in the lab would be conducted in this study. Repeated cyclic loading that causes significant plastic strains after a

relatively small number of cycles, e.g., hundreds or thousands called LCF or a relatively large number of cycles named HCF even though there in no arbitrary loading-cycle classifying two regimes.

In the low and high cycle fatigue tests in this study, the 4PB tests are performed on the beam specimens under various cyclic vertical displacement levels equivalent to strain amplitudes. The specimen is forced to follow given variable amplitudes, cyclic strains afterwards. The stress-response of the material during cycling is monitored and the number of loading cycles to failure is recorded for each specimen. Results of all tests are utilized to explain the fatigue behavior of 13-mm dense graded HMA in the regimes of LCF and HCF phenomenologically in this study.[14][15]

Dissipated Energy during Loading Cycle

Fatigue damage may be correlated with the amount of dissipated energy in the specimen during loading cycle. The dissipated energy, which is intrinsic components of the loss part of the total potential energy of the specimen, can be used to explain either the decrease in flexural stiffness or the incremental change in fatigue damage during a 4PB testing.[4]

To present the hysteresis loop during the repetitive cyclic loading for the 13mm dense-graded HMA in this study, test results with the maximum constant strain amplitude about 500$\mu\varepsilon$ are representing the stress versus strain history per 1,000 cycles in Figure 3 as an example. The stiffness of the specimen is decreasing as the loading cycle is increasing until the specimen is completely failed after 9,800 cycles within this case. During the whole loading cycles to the failure, the specimen may experience the three regimes of the fatigue behavior aforementioned.

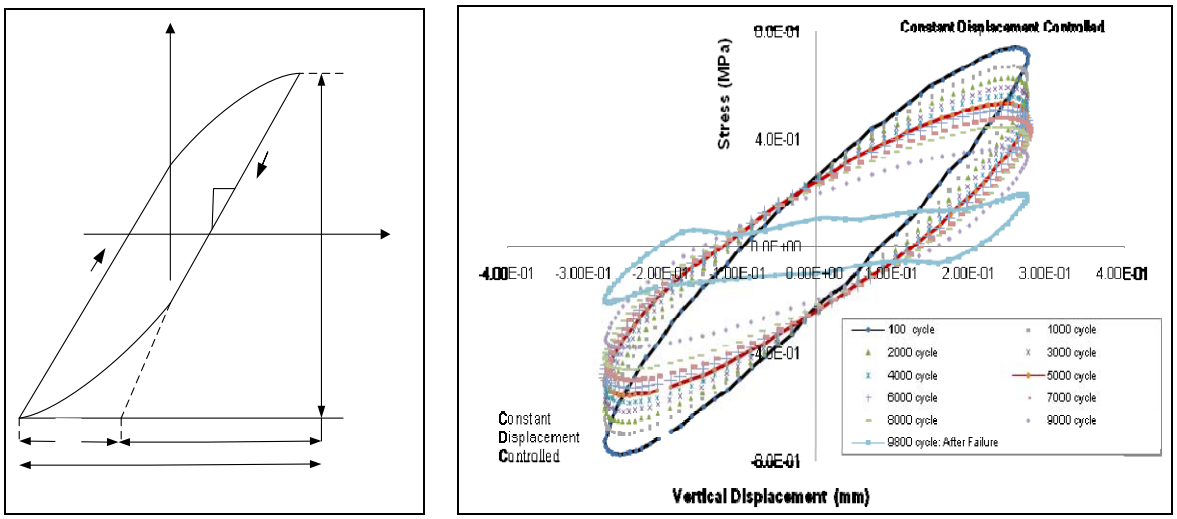

(a) (b)

Figure 3. ; (a) Conceptual cyclic stress-strain hysteresis loop; (b) Cyclic stress-strain hysteresis loop of 13mm dense graded HMA

From the conceptual strain-stress hysteresis loop, Figure 3a, if the stress and strain variation for one cycle is plotted, a closed hysteresis loop is formed on each cycle. The total strain can be separated into the elastic strain, $\Delta\varepsilon_e$, and plastic one, $\Delta\varepsilon_p$.[14]

Moreover, the dissipated energy changes calculated from a hysteresis loop (Figure 3b) being taken near end of the stable region (secondary stage) are utilized to represent the threshold of fatigue failure being discussed following sections in more detail. During the cyclic loading in the 4PB fatigue test, the fatigue damage may be characterized by the dissipated strain energy of the specimen. The rate of dissipated energy change follows a primary stage, the rate of the dissipated energy decrease gradually, then remains nearly constant for a while within the secondary stage, and finally accelerates again until the specimen fails as shown in the concept drawing of Figure 4. The fatigue damage is revealed by a sudden change of the rate of the dissipated energy.

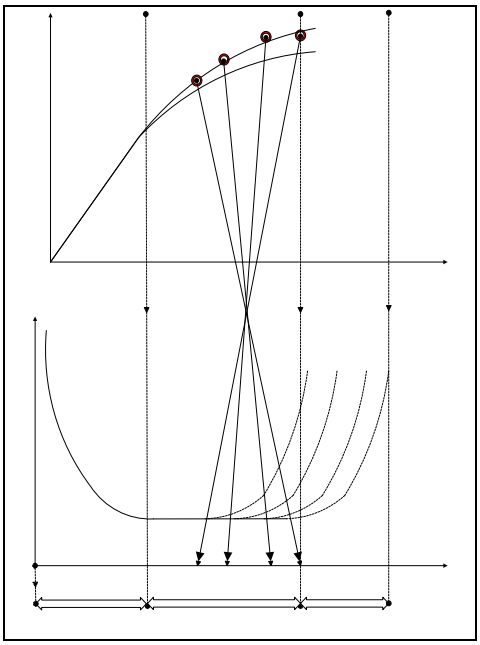

Figure 4. (a) Cyclic Stress-Strain behavior and (b) Ratio of Dissipated Energy Change versus Loading Cycles (N_f)

The four dots in Figure 4 (a) represent that the stress amplitude versus strain amplitude near end of the stable region (secondary stage) where a sudden change of the rate of the dissipated energy occurs in Figure 4 (b)(N_f-I, N_f-II, N_f-III, and N_f-IV). If relatively higher constant strain amplitudes or loading rate are applied to the specimen, this may result in relatively shorter fatigue life of N_f in Figure 4(b). The transition point is where the stable region evolves into the plastic region. To build these graphs, first, we need to calculate the dissipated energy during a loading cycle usually in 100 loading cycle-interval for convenience, then, the relative ratio of the dissipated energy change would be computed by following procedures.

The dissipated energy per unit volume per cycle or period time is determined as following equation deriving from total potential energy per loading cycle.[16]

$$\therefore\ W_i = Dissipated \quad Energy \quad (DE) = \pi \hat{\varepsilon}^2 E''(w) = \pi \hat{\varepsilon}^2 \left| E^* \right| \sin \delta = \pi \hat{\varepsilon}_i \sigma_i \sin \delta_i \tag{9}$$

where

W_i = dissipated energy at load cycle i,

$E''(w)$ = loss part of Modulus

σ_i = stress amplitude at load cycle i,

$\hat{\varepsilon}_i$ = strain amplitude at load cycle i, and

δ_i = phase angle between stress and strain wave signals.

All the dissipated energy per cycle is computed by using the Equation (9) in this study, where DE is the dissipated energy per cycle, expressed in Pa. The cumulative dissipated energy was then determined by summing the dissipated energy per cycle over the fatigue life of the specimen. Through the Equation (9), one can find a direct reference to energy dissipation involving products of stress and strain.

Ghuzlan and Carpenter (2000) propose to use the ratio of dissipated energy change per predefined cycle, usually 100 cycle interval, related to the dissipated energy per cycle as a measure of fatigue failure. The ratio of dissipated energy change (RDEC) per predefined cyclic interval can be calculated by the Equation (10):[4]

$$RDEC_a = \left| \frac{DE_a - DE_b}{DE_a \times (b-a)} \right| \tag{11}$$

where
RDEC= the ratio of dissipated energy change,
a, b = loading cycles, 100 cyclic interval, and
DE = dissipated energy during a loading cycle a and b respectively.

The RDEC of the 13mm dense-grade HMA is plotted versus the number of load cycles to characterize the mixture's fatigue behavior in Figures 5a and b as an example in this study. They are representing that the RDEC rapidly changes during the primary stage of loading cycle until the most cycle-dependent hardening or softening is complete. Following the primary stage, the curve remains relatively constant indicating the stable fatigue damage resistance as a secondary stage of the fatigue. Upon failure, the RDEC rapidly increases again and much larger portion of the dissipated energy capacity of the specimen may be converting to the fatigue damage representing the tertiary stage shown in Figure 5a and 5b.

In this case, the fatigue failure of the 13mm dense-graded HMA specimen under the 500 με of the strain amplitude is defined as the number of loading cycles about 8,000 repetitions wherein the RDEC begins to increase successively, which is not the loading cycle when the initial stiffness reaches to the value of 50% of initial stiffness like N_f-50%.

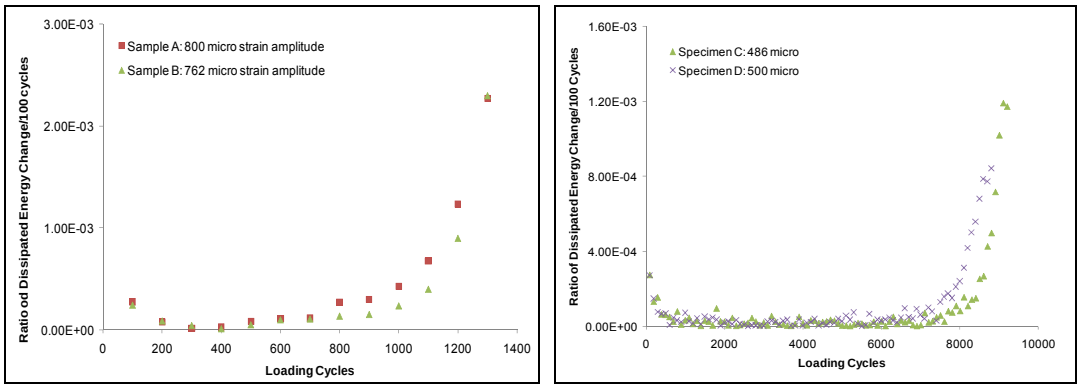

(a) (b)

Figure 5. History of RDEC of 13mm-Dense graded HMA; (a) strain amplitude about 800με, and (b) strain amplitude about 500με

To present that the conventional N_f-50% criterion for the fatigue failure threshold is not valid for all tests in this study, the x-axis of the Figure 6 represents the various strain amplitudes for all tests and the y-axis takes the values of the specimen's stiffness of; (1) the initial cyclic loading (initial stiffness after 50 loading cycles), (2) the fatigue failure defining RDEC change after a large number of loading cycles (stiffness at the failure), and (3) the 50% of initial stiffness(50% of initial stiffness) respectively.

As shown in Figure 6 for the 4PB results of 13mm dense-graded HMA in this study, it is not enough to address the fatigue failure at the loading cycle when the initial stiffness reaches to the 50% of its initial stiffness, because almost all specimens maintain some values of stiffness above the 50% of initial stiffness at the fatigue failure threshold at which is defined by using the RDEC change as arguing above.

Thus, the limit cycle of fatigue resistance or fatigue failure (N_f) of each specimen in this study is represented by a number of loading cycle nearby the end of the stable region where the RDEC starts increasing again to the end of each test successively.

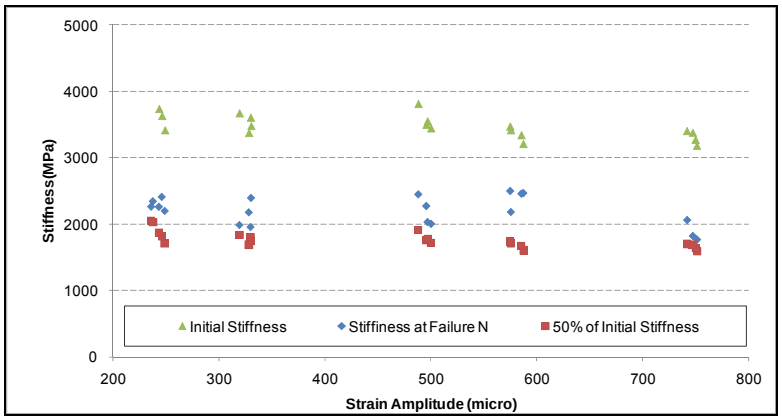

Figure 6. Stiffness Changes of the 13mm dense-graded HMA

4. CONCLUSION

The main idea of this study based on the conventional fatigue analysis of HMA done by many well-known research groups leading by C. Monismith and S. Carpenter. The conventional fatigue analysis of HMA is that the fatigue damage is accumulated during cyclic loadings until to the predefined fatigue failure criterion like N_f-50%.

The accumulated fatigue damage may result in micro or macro fatigue damages depending on the magnitude of the applied strain or stress amplitudes on the four point bending beam specimens. This means that the fatigue cracks or damages may be developed in two different strain-controlled modes; one is low cycle fatigue damage developed by the relative high strain amplitudes, and the other is high cycle fatigue damages in relatively low strain amplitudes.

The main focus of the conventional fatigue approach is on modeling a fatigue life transfer function to correlate between the number of loading cycle governed by the predefined failure criterion (N_f-50% rule) and strain amplitude, initial stiffness, or cumulative dissipated energy. Although the conventional fatigue life transfer function can be widely used to calculate the number of loading cycle to fatigue failure in the process of pavement thickness design, it does not provide relative measures to quantify the elastic strains and plastic strains phenomenologically depending on the strain amplitudes except the endurance limit of strain.

This study gives an alternative approach to define the predefined fatigue failure criterion using the ratio of the dissipated energy change instead of using the conventional N_f-50% criterion.

In conclusion, the dense-graded 13mm HMA specimens were tested using four-point bending fixture at various strain amplitudes (200$\mu\varepsilon$-800$\mu\varepsilon$) under the strain-controlled mode at 20°C. This study clarifies that the dissipated energy change during the whole loading cycles exhibits the three typical stages of fatigue behavior such as the primary, steady-state, and tertiary stages. On these three stages, a new threshold of fatigue failure between the steady-state (secondary stage) and the tertiary stage was utilized to explain the fatigue behavior of HMA using ration of dissipated-energy change. In other words, a promising fatigue life prediction threshold, N_f, is proposed as a fatigue life transition point where the stable fatigue behavior evolved into the fatigue failure, which is a allowable loading repetition up to the possible macro damage or crack initiation.

Authors will do more tests with various mixtures, temperatures, and loading conditions to propose a fundamental measure for the pavement thickness design utilizing the Coffin-Manson as a future research. And also, in the future, the effects of loading frequency and rest periods on the fatigue behavior will be addressed in fatigue evaluation through this approach.

REFERENCES

1. Pyeong Jun Yoo and I. L. Al-Qadi. The truth and myth of fatigue cracking potential in Hot-Mix Asphalt: numerical analysis and validation. the Journal of the AAPT. Vol 77. pp 549-590. 2008

2. S.H. Carpenter. Fatigue performance of IDOT mixtures. IHR/ICT R39. Illinois Center for Transportation. 2006

3. C. L. Monismith and J.A. Deacon. Fatigue of asphalt paving mixtures. Vol 95. No. TE2. Transportation Engineering Journal. American Society of Civil Engineers. USA. 1969

4. Shen S. and S.H. Carpenter. Application of dissipated energy concept in fatigue endurance limit testing. TRR1929. pp165-173. TRB. National Research Council. Washington. DC. 2005

5. A. Constantinescu. et al. A unified approach for high and low cycle fatigue based on shakedown concepts. Vol 26. pp 561-568. Fatigue Fracture Engineering Material and Structure. Blackwell Pub lLtd. 2003

6. A. C. Pronk. Four point dynamic bending test. DWW-96-088. pp23-27. Road and Hydraulic Division. Netherlands. 2006

7. I.L. Al-Qadi. et al. Fatigue life characterization of superpave mixtures at the Virginia Smart Road, Final Contract Report No. FHWA/VTRC 06-CR1. pp60-75. Charlottesville. VA. 2005

8. J. T. Harvey. et al. Evaluation of fatigue and permanent deformation properties of several asphalt-aggregate field mixes using strategic highway research program A-003A Equipment. TRR 1454. pp. 123-133., TRB. National Research Coauncil. Washington. DC. 1994.

9. C.L. Monismith. et al. Asphalt mixturebehavior in repeated flexture. Report No. TE70-5. Institute of Transportation and Traffic Engineering. University of California. Berkeley. 1972

10. D.H. Timm and D.E. Newcomb. Calibration of flexible pavement performance equations. TRR 1853. pp. 134-142. TRB. National Research Council. Washington. DC. 2003

11. F. Finn. et al. Development of pavement structural subsystems., NCHRP Report 291. TRB. Washington. D.C. 1986

12. A. Tayebali. et.al. Mixture and mode-of-loading effects on fatigue response of asphalt-aggregate mixtures. vol. 63. pp118-151. Proceedings of the Association of Asphalt Paving Technologists. 1994

13. Strategic Highway Research Program. Fatigue Response of asphalt-aggregate mixes. SHRP-A-404. National Research Council. Washington. DC. USA. 1994

14. N.E. Dowling. Mechanical behavior of materials. Second Enition. pp 649. Prentice Hall. USA. 1999

15. Altug Erberik and Haluk Sucuoglu. Seismic energy dissipation in deteriorating systems through low-cycle fatigue. Vol 33. pp 49-67. Earthquake Engineering and Structural Dynamics. John Wiley & Sons. Ltd. 2004

16. D.A. Dillard. Phenomenological viscoelasticity of polymers. Engineering Science and Mechanics Hand-book. pp10-30. Virginia Tech. Blacksberg. VA. 1999